Effect of Spatial Modulated Light on Position of Self-Calibration Point

Idit Feder, Hamootal Duadi, and Dror Fixler

***Abstract*—In optical sensing, the differentiation between absorption and scattering poses a challenge when dealing with a physiological medium. We have shown that for extracting absorption-based parameters it is optimal to measure at the iso-path length (IPL) point. The IPL position is dependent on the diameter of the medium. In this paper, we will demonstrate how beam shaping can help match the light pattern, so the IPL point remains in the same position and distance from the light source. Hence, the location of the detector will remain constant for different mediums, such as different fingers. A spatial frequency of 0.4 mm^{-1}, in the case of a 15mm diameter cylindrical phantoms, shifts the IPL point's position by 40 degrees on the phantom's surface. Moreover, the spatial modulation yields an optical signature from different depths, which could improve the extraction of optical properties from tissue depth using our method.**

***Index Terms*—Absorption, biomedical engineering, optical modulation, phantoms, scattering parameters.**

I. Introduction

SENSING biological tissues using noninvasive optical methods is a quick and safe way to characterize them. The tissue components scatter and absorb light, so the reemitted light constitutes an optical signature of its content. However, the extraction of optical parameters is a challenge due to the combined influences of scattering and absorption. The changes of the scattering coefficient (μ_s) and absorption coefficient (μ_a) in tissues can predict an early change in the physiological state [1]. To better characterize the tissue states, optical methods can incorporate modulated illumination. The advantage of spatially modulated illumination is the ability to extract both optical properties and depth information from the reflectance of a heterogenic turbid medium [2]–[4]. To control the depth inside the turbid medium, the illumination pattern is modified to various spatial frequencies. For example, for a sinusoidally varying illumination, the source is described by the following equation:

$$s = s_0 \left(\frac{1}{2} \sin\left(2\pi f_x + \alpha\right) + \frac{1}{2} \right) \tag{1}$$

where f_x is the spatial frequency of the sinusoid and α is the spatial phase. Using the time-independent diffusion equation result for this sinusoidal source, the new effective attenuation coefficient (μ_{eff}) is obtained in Eq. 2. This parameter determines the effective penetration depth ($\delta_{eff} = 1/\mu_{eff}$), which in this case depends on the spatial frequency. Hence, the spatial structure changes the penetration depth.

$$\mu_{eff} = \sqrt{3\mu_a \left(\mu_s' + \mu_a\right) + \left(2\pi f_x x\right)^2} \tag{2}$$

In addition, high frequency (f_x>0.25 mm^{-1}) diffused reflectance is more sensitive to scattering than absorption, whereas lower spatial frequency patterns are mainly sensitive to absorption [5]–[7]. Therefore, in cases where scattering or sensitivity to superficial layers is important, a higher frequency can be used. When examining deeper layers, lower frequencies can be used. Studies that deal with the characterization of turbid media use spatial frequency domain reflectometry (SFDR) or spatial frequency domain imaging (SFDI) techniques achieve an accurate determination of the optical properties and depth-resolved imaging [4]. These achievements are relevant to a wide range of biomedical health applications [8], [9]. For example, Dognitz [3] measured the optical coefficients of human skin *in vivo* using an illumination pattern of dark and bright concentric rings of equal width with the SFDR method. Moreover, by the SFDI method, Cuccia [4] reported wide-field imaging of quantitative optical properties of a heterogeneous phantom. *In vivo* depth-resolved imaging was presented by Abookasis [10] through a thinned rat skull. He used spatial modulation to detect and map changes in both optical properties and tissue composition. Furthermore, SFDI of brain tissue and measurements of neural tissue function were reported by Lin [11]. Weber [5] improved SFDI by combining multiple spatial frequency domain imaging with a computed-tomography imaging spectrometer. To increase SFDI data acquisition speed, Nadeau [7] used binary square wave patterns to generate absorption and reduced scattering maps, faster than sinusoids typically used in SFDI. Optimization of the frequency parameter was reported by Bodenschatz [6] and Hu [12] for spatial frequency imaging of biological materials. The widespread use of spatial modulation for mapping turbid media in different optical techniques, with its potential applications in human disease (ischemic stroke [10], Alzheimer's disease [11] and cerebral edema [13], etc.), led us to examine the modulation effect on our method.

In previous studies, we presented our unique method. The full scattering profile (FSP) describes the medium by its circumferential signature, the angular light distribution when illuminated by a single wavelength. So, the reflected light is measured as well

Manuscript received June 7, 2021; revised June 29, 2021; accepted July 1, 2021. Date of publication July 8, 2021; date of current version August 18, 2021. *(Corresponding author: Dror Fixler.)*

The authors are with the Faculty of Engineering and the Institute of Nanotechnology and Advanced Materials, Bar Ilan University, Ramat Gan 5290002, Israel (e-mail: iditdag@gmail.com; hamootal@gmail.com; dror.fixler@biu.ac.il).

Digital Object Identifier 10.1109/JPHOT.2021.3094722

as the transmitted light. The common modulation techniques, as mentioned above, focus on the reflected light only. The novelty of our examination is the iso-path length (IPL) point phenomenon [14]–[16]. At this point, the light intensity is not influenced by the scattering components of the medium. The scattering neutralization adds accuracy for the optical sensing of a biological medium that is based on absorption properties.

The method was well established by Monta Carlo simulations and measured in tissue-like phantoms. The FSPs and the IPL point were examined using phantoms with different materials: liquid phantoms based on Intra-Lipids and solid phantoms with Agarose, PDMS, or silicon [16]. In addition, *in vivo* measurements on fingers with different diameters and mice were presented [17], [18]. We showed that the IPL phenomenon occurs in different geometries: in cylindrical mediums, with circular and elliptical cross-sections, as well as semi-infinite mediums [17], [19]. In the case of cylindrical phantoms, the linear dependency between the medium diameter and the IPL point's position was found [15]. Hence, for each person, the IPL point has a specific position depended on his finger diameter. Moreover, the same blood volume with different distributions inside the medium was investigated [20], and the shielding effect was overcome; The FSP was influenced by the scattering as well the absorption of blood, but the IPL point remained constant despite the changes in different physiological states. These findings can be useful for a wide range of measurements in the biosensing field.

This paper focuses on the influence of spatially modulated light on the FSP, and especially on the IPL point. In physiological parameters measurements, the detector is commonly located on the finger that often changes, which repositions the calibration point. We present the FSPs of cylindrical phantoms with various scattering coefficients and in different diameters, obtained by modulated light irradiation. The combination between the FSP method and the modulation approach is required to maximize the capabilities of the method and overcome changes in diameter in the case of a given detector location.

II. Material and Methods

A. The Optical System

We built a unique optical system for measuring the FSP (Fig. 1a). A green Nd:YAG laser at a wavelength of 532nm was used as an excitation source to illuminate the sample after passing through a printed mask to spatially modulate the light. We used the NIR regime in our previous works [20], [21] because of the penetration depth into the tissue. However, for applications with a higher signal-to-noise ratio, it is common to use a green light source for clinical measurements [22], for example for extracting pulse rate in PPG. To adjust our method for a wide range of applications we worked in this study with a green light source. The light that passes through the sample was measured using a photodiode (PD, SM05 Thorlabs) with an active area of 13mm^2, which collected the light intensity. The PD was positioned on a rotation stage, so the distance from the phantom's surface was constant (2.5cm) and the measurement was performed in various exit angles relative to the entrance point. The measurement angle was defined to be 0 degrees for the ballistic photons that have not experienced scattering, whereas 180 degrees was defined as the laser direction.

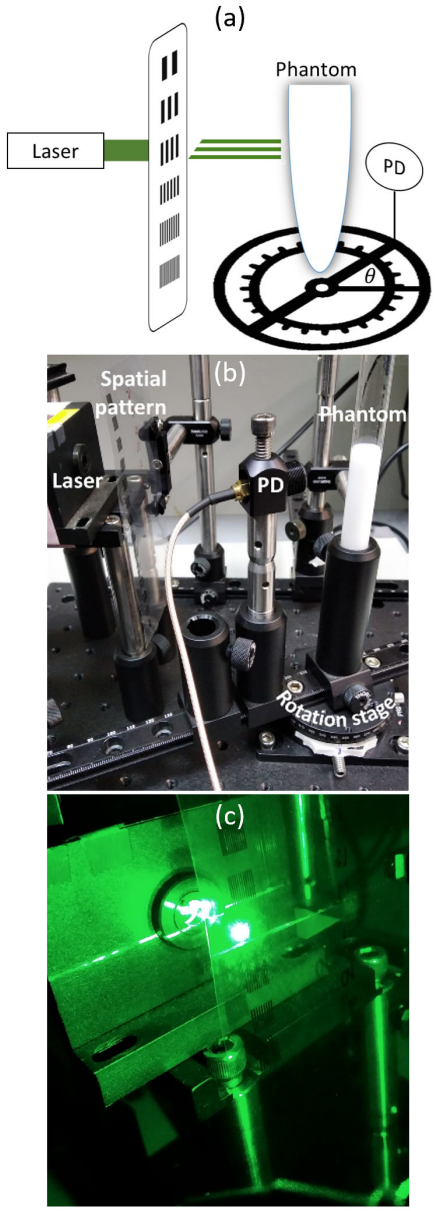

Fig. 1. (a) A scheme of the system for measuring the FSP with spatially modulated light, (b) a picture of the experimental setup and (c) the patterns of the modulation.

The masks consisted of vertical line patterns with different spatial frequencies (0 to 0.45 mm^{-1}), and a duty cycle of 50% so the total light intensity remained constant, as measured by a photodetector (NOVA II, Ophir). The masks which are presented in Fig. 1c were illuminated by the laser. Before placing the phantom, a CMOS camera (Thorlabs) was positioned in the entrance point to the phantom to verify the illumination pattern. After verifying the modulation, the cylindrical phantoms were placed. The vertical lines of the mask were aligned with the longitudinal axis of the cylinder.

TABLE I
PHANTOMS SCATTERING COEFFICIENTS

%IL	μ'_s [cm^{-1}]
0.828	18
0.921	20
1.105	24
1.197	26

B. Solid Phantoms

Solid phantoms with different reduced scattering coefficients as well as different diameters were measured. The reduced scattering coefficient is defined as $\mu'_s = \mu_s(1\text{-}g)$, where g is the anisotropy factor. The phantom contains Intra Lipid (IL, IntraLipid 20% Emulsion, Sigma-Aldrich, Israel) as a scattering component and 1% agarose powder (SeaKem LE Agarose, Ornat, Israel) for solidification. The phantoms' scattering coefficients are determined by the IL concentration in the range of 18 cm^{-1}–26 cm^{-1} (Table I). Initially, we prepared a solution with 2% agarose powder melted in double-distilled water (slowly added at ~70°C temperature). Then it was mixed with IL in various concertations diluted in double-distilled water. The final solution was poured into glass tubes of different diameters (13mm and 15mm).

III. RESULTS

A. Comparison of FSPs With and Without Spatial Modulation

To examine the influence of spatial modulation on the FSP, we measured the FSP of solid phantoms with different reduced scattering coefficients between 18cm^{-1} to 26cm^{-1}. They were irradiated by a gaussian beam from the laser in comparison to a spatially modulated beam (with spatial frequencies 0-0.45 mm^{-1}). The experimental results of the 13mm diameter phantom are presented in Fig. 2. We found the IPL point at 135 degrees before adding any modulation (Fig. 2(a)). In our previous publications [14] in 13mm diameter, we found the IPL position at 117 degrees. However, in our recent publication [23], we showed that a factor of 16 increment in detector size, (13mm^2 compared to 0.8mm^2) shifts the IPL position by 15 degrees. Moreover, a small change in the distance of the detector from the phantom's surface may explain the additional 3 degrees shift in the IPL position.

Next, the phantoms were measured using the spatially modulated light, for example, the FSPs for an input light beam with a frequency of 0.416 mm^{-1} are presented in Fig. 2b, there the IPL point shifts to 110 degrees.

Similar behavior occurs in the larger diameter. The FSPs of the phantoms with 15 mm diameter are presented in Fig. 3. The IPL point appears at 145 degrees for a regular Gaussian laser (Fig. 3a), whereas for the modulated source, with a frequency of 0.416 cm^{-1} the IPL point shifts to 105 degrees (Fig. 3b). The IPL position of the larger diameter without modulation is higher than the IPL position of the smaller diameter phantoms, as we have shown in previous works [15]. Nevertheless, with modulated light, the IPL point phenomenon remains, which is important as a self-calibration point.

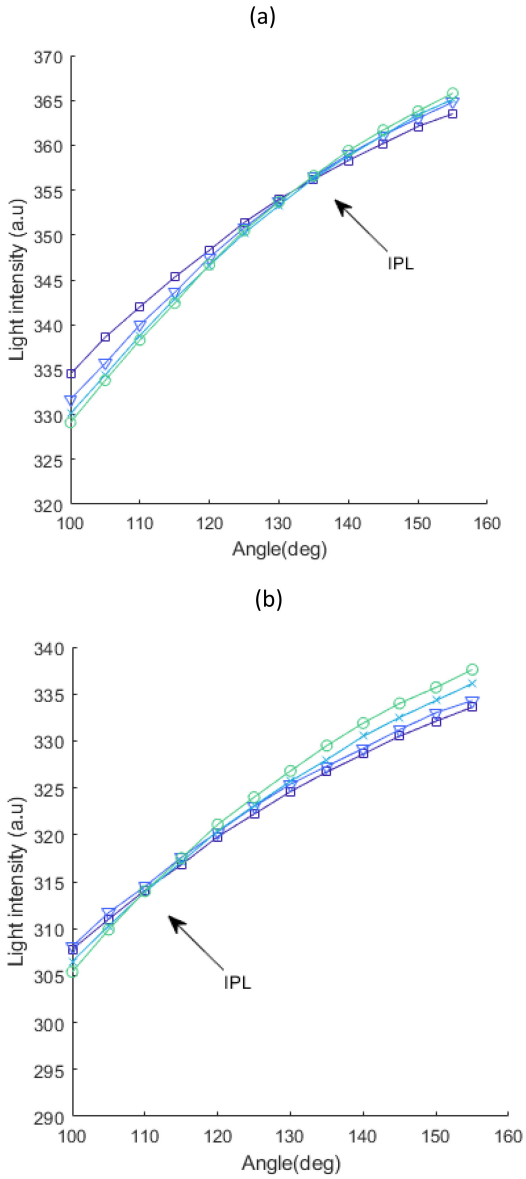

Fig. 2. Comparison of FSPs with and without spatial modulation for phantoms with a 13 mm diameter. (a) FSPs of illumination without modulation and (b) FSPs of spatial modulation with a frequency of 0.416 mm^{-1}. Each curve represents a FSP of a phantom with different reduced scattering coefficients (square, triangle, x, and circles for 18,20,24,26 cm^{-1} respectively). The IPL point shifted from 135 degrees to 110 degrees due to the modulation.

B. Position of Self-Calibration Point

Several frequencies of modulation were examined. The shifting of the IPL point's position where according to the spatial frequency. As the frequency increases the IPL point's angle moves further from the light entry point, as presented in Fig. 4. This was expected since the light penetration depth shortens with the increase of the spatial frequency. Hence, the IPL point that represents a specific optical path length (OPL) moved away from the light source. The ability to shift this calibration point by the modulation parameters can be useful to calibrate the system in a specific angle that is set arbitrarily due to technical constraints.

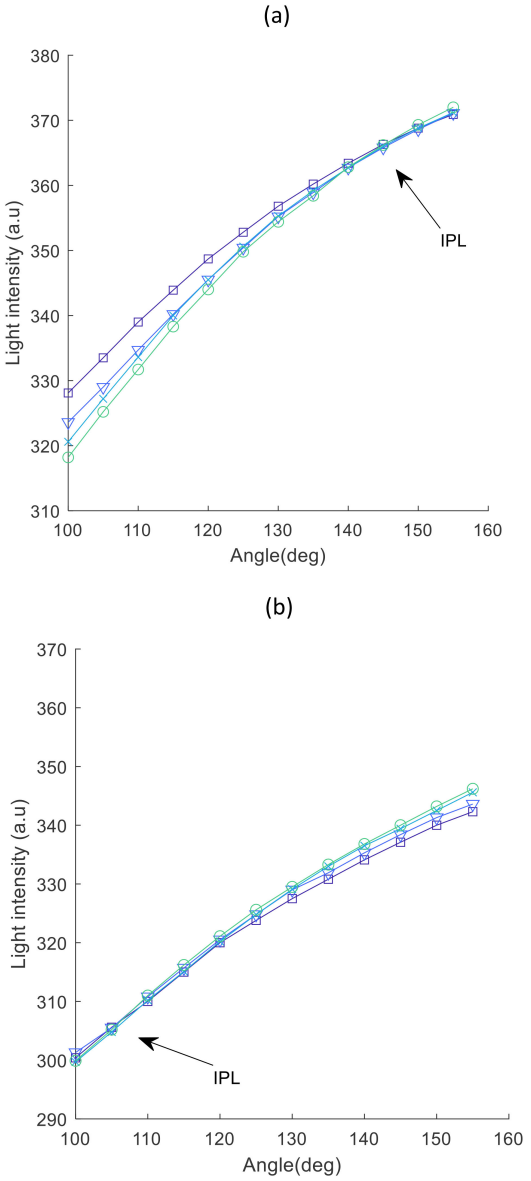

Fig. 3. Comparison of FSPs with and without spatial modulation for phantoms with a 15mm diameter. (a) FSPs of illumination without modulation and (b) FSPs of spatial modulation with a frequency of 0.416 mm^{-1}. Each curve represents a FSP of a phantom with a different reduced scattering coefficient (square, triangle, x, and circles for 18,20,24,26 cm^{-1} respectively). The IPL point shifted from 145 degrees to 105 degrees due to the modulation.

For example, in the case of a device that has a detector that is already located, or for a tissue that changed diameter.

IV. Discussion

FSPs of phantoms with different scattering coefficients were presented, illuminated without modulation. There, the position of the IPL point is in accordance with the different diameters; for the larger diameter a higher angle position was found, where the higher angles are closer to the source. Next, using modulated light, the FSPs were measured, and the IPL point was presented. In comparison to the non-modulated light, the IPL point's position was in a lower angle for the larger diameter. The change in

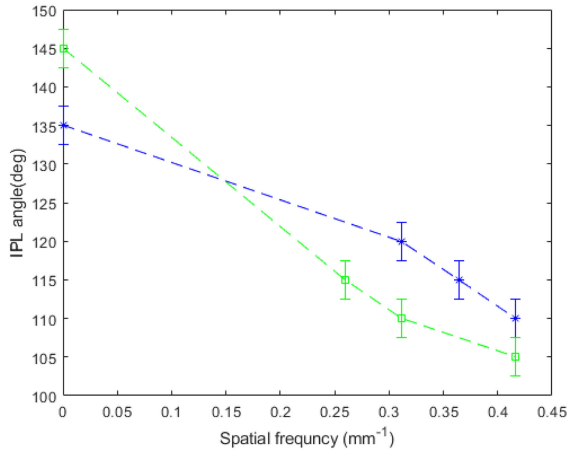

Fig. 4. The IPL position shifts as a function of spatial modulation. Measurements of phantoms with a 15 mm diameter presented in squares and 13mm diameter in stars.

the IPL point as a function of the spatial modulated frequency stems from the change of the OPL. The phantoms, as in tissues, behave like a low-pass filter, hence as the spatial frequency increases the reflectance reduces [4]. For higher frequencies, the OPL is shorter. In larger diameters, this shortening is more significant. The curves of the IPL position as a function of the spatial frequency have a common point; at that point for a specific frequency, the same IPL position is obtained. It might be useful for measuring with a detector that is localized at a certain distance from the surface and measuring samples with various diameters.

V. Conclusion

This paper deals with the effects of modulated light on the FSP method. The FSPs of phantoms with a range of reduced scattering coefficients in different diameters were measured. The optical signature of these cylindrical turbid media was examined using patterns of light and dark stripes, which are projected at different spatial frequencies. The innovation of this study is the light modulation, in comparison to previous works that we presented a light source with a Gaussian beam without spatial modulation. The IPL point phenomenon exists even with the changing of the illumination pattern. The different spatial frequencies shift the position of the IPL point. The OPL changes after modulation, so the IPL appears in a different location on the surface. Hence it can be useful to utilize an arbitrary IPL point, determined by a given distance between the source and the detector, for objects with different diameters by changing the spatial frequency. In other words, instead of changing the device for each person, with its precision limitations, one can use spatial modulation to shift the IPL position as much as needed. Furthermore, wavefront shaping in our optical system will achieve FSPs of cylindrical tissues influenced by different depths that is relevant for imaging and tomography methods. In addition, the implantation of this method for the detection of personalized physiological changes, based on absorbance measurements, could add to the accuracy of personalized detection.

ACKNOWLEDGMENT

The authors wish to thank Israel Science Foundation (ISF) for their funding (1195/18).

REFERENCES

[1] S. L. Jacques, "Optical properties of biological tissues: A review," *Phys. Med. Biol.*, vol. 58, pp. R37–61, 2013, doi: 10.1088/0031-9155/58/11/R37.

[2] F. Bevilacqua, D. Piguet, P. Marquet, J. D. Gross, B. J. Tromberg, and C. Depeursinge, "In vivo local determination of tissue optical properties: Applications to human brain," *Appl. Opt.*, vol. 38, no. 22, 1999, Art. no. 4939, doi: 10.1364/ao.38.004939.

[3] N. Dögnitz and G. Wagnières, "Determination of tissue optical properties by steady-state spatial frequency-domain reflectometry," *Lasers Med. Sci.*, vol. 13, no. 1, pp. 55–65, 1998, doi: 10.1007/BF00592960.

[4] D. J. Cuccia, F. Bevilacqua, A. J. Durkin, and B. J. Tromberg, "Modulated imaging: Quantitative analysis and tomography of turbid media in the spatial-frequency domain," *Opt. Lett.*, vol. 30, no. 11, 2005, Art. no. 1354, doi: 10.1364/ol.30.001354.

[5] J. R. Weber *et al.*, "Multispectral imaging of tissue absorption and scattering using spatial frequency domain imaging and a computed-tomography imaging spectrometer," *J. Biomed. Opt.*, vol. 16, no. 1, 2011, Art. no. 011015, doi: 10.1117/1.3528628.

[6] N. Bodenschatz, P. Krauter, A. Liemert, J. Wiest, and A. Kienle, "Model-based analysis on the influence of spatial frequency selection in spatial frequency domain imaging," *Appl. Opt.*, vol. 54, no. 22, 2015, Art. no. 6725, doi: 10.1364/ao.54.006725.

[7] K. P. Nadeau, T. B. Rice, A. J. Durkin, and B. J. Tromberg, "Multifrequency synthesis and extraction using square wave projection patterns for quantitative tissue imaging," *J. Biomed. Opt.*, vol. 20, no. 11, 2015, Art. no. 116005, doi: 10.1117/1.jbo.20.11.116005.

[8] J. R. Weber, D. J. Cuccia, A. J. Durkin, and B. J. Tromberg, "Non-contact imaging of absorption and scattering in layered tissue using spatially modulated structured light," *J. Appl. Phys.*, vol. 105, no. 10, pp. 102028-1–102028-9, 2009, doi: 10.1063/1.3116135.

[9] R. Rowland *et al.*, "Burn wound classification model using spatial frequency-domain imaging and machine learning," *J. Biomed. Opt.*, vol. 24, no. 5, pp. 056007-1–056007-9, 2019, doi: 10.1117/1.jbo.24.5.056007.

[10] D. Abookasis, C. C. Lay, M. S. Mathews, M. E. Linskey, R. D. Frostig, and B. J. Tromberg, "Imaging cortical absorption, scattering, and hemodynamic response during ischemic stroke using spatially modulated near-infrared illumination," *J. Biomed. Opt.*, vol. 14, no. 2, 2009, Art. no. 024033, doi: 10.1117/1.3116709.

[11] A. J. Lin *et al.*, "Spatial frequency domain imaging of intrinsic optical property contrast in a mouse model of Alzheimer's disease," *Ann. Biomed. Eng.*, vol. 39, no. 4, pp. 1349–1357, 2011, doi: 10.1007/s10439-011-0269-6.

[12] D. Hu, R. Lu, and Y. Ying, "A two-step parameter optimization algorithm for improving estimation of optical properties using spatial frequency domain imaging," *J. Quant. Spectrosc. Radiat. Transf.*, vol. 207, pp. 32–40, 2018, doi: 10.1016/j.jqsrt.2017.12.022.

[13] D. Abookasis *et al.*, "Using NIR spatial illumination for detection and mapping chromophore changes during cerebral edema," *Photonic Ther. Diagnostics IV*, vol. 6842, no. June 2014, 2008, Art. no. 68422U, doi: 10.1117/12.760516.

[14] I. Feder, H. Duadi, and D. Fixler, "Experimental system for measuring the full scattering profile of circular phantoms," *Biomed. Opt. Expr.*, vol. 6, no. 8, 2015, Art. no. 2877, doi: 10.1364/boe.6.002877.

[15] H. Duadi, I. Feder, and D. Fixler, "Linear dependency of full scattering profile isobaric point on tissue diameter," *J. Biomed. Opt.*, vol. 19, no. 2, 2014, Art. no. 026007, doi: 10.1117/1.jbo.19.2.026007.

[16] I. Feder, M. Wróbel, H. Duadi, M. Jędrzejewska-Szczerska, and D. Fixler, "Experimental results of full scattering profile from finger tissue-like phantom," *Biomed. Opt. Exp.*, vol. 7, no. 11, 2016, Art. no. 4695, doi: 10.1364/boe.7.004695.

[17] H. Duadi, I. Feder, and D. Fixler, "Near-infrared human finger measurements based on self-calibration point: Simulation and in vivo experiments," *J. Biophotonics*, vol. 11, no. 4, 2018, doi: 10.1002/jbio.201700208.

[18] H. D. and D. Fixler, "Influence of multiple scattering and absorption on the full scattering profile and the isobaric point in tissue Hamootal," *J. Biomed. Opt.*, vol. 20, no. 5, 2015, Art. no. 056010, doi: 10.1117/1.JBO.20.5.056010.

[19] I. Feder, H. Duadi, R. Chakraborty, and D. Fixler, "Self-calibration phenomenon for near-infrared clinical measurements: Theory, simulation, and experiments," *ACS Omega*, vol. 3, no. 3, pp. 2837–2844, 2018, doi: 10.1021/acsomega.8b00018.

[20] I. Feder, H. Duadi, T. Dreifuss, and D. Fixler, "The influence of the blood vessel diameter on the full scattering profile from cylindrical tissues: Experimental evidence for the shielding effect," *J. Biophotonics*, vol. 9, no. 10, pp. 1001–1008, 2016, doi: 10.1002/jbio.201500218.

[21] I. Feder, H. Duadi, M. Fridman, T. Dreifuss, and D. Fixler, "Experimentally testing the role of blood vessels in the full scattering profile: Solid phantom measurements," *J. Biomed. Photon. Eng.*, vol. 2, no. 4, 2016, Art. no. 040301, doi: 10.18287/jbpe16.02.040301.

[22] Y. C. Lin and Y. H. Lin, "A study of color illumination effect on the SNR of rPPG signals," in *Proc. Annu. Int. Conf. IEEE Eng. Med. Biol. Soc. EMBS*, 2017, no. July 2017, pp. 4301–4304, doi: 10.1109/EMBC.2017.8037807.

[23] H. Duadi, I. Feder, and D. Fixler, "Influence of detector size and positioning on near-infrared measurements and ISO-pathlength point of turbid materials," *Front. Phys.*, vol. 9, no. Mar., pp. 1–6, 2021, doi: 10.3389/fphy.2021.647281.